Int. J. Electrochem. Sci., 10 **(2015)** 4090 - 4096

International Journal of
ELECTROCHEMICAL
SCIENCE
www.electrochemsci.org

Short Communication

Performance of $LiCu_xMn_{2-x}O_4(0\leq x\leq 0.10)$ Cathode Materials Prepared by a Fameless Combustion Synthesis

Jiabin Hao[1,2], *Lei Zhong*[1,2], *Jintao Liu*[1,2], *Fangli Yang*[1,2], *Hongli Bai*[1,2], *Changwei Su*[1,2], *Junming Guo*[1,2,*]

[1] Engineering Research Center of Biopolymer Functional Materials of Yunnan, Yunnan Minzu University, Kunming 650500, PR China
[2] Key Laboratory of Chemistry in Ethnic Medicinal Resources, State Ethnic Affairs Commission & Ministry of Education, Yunnan Minzu University, Kunming 650500, PR China
[*]E-mail: guojunming@tsinghua.org.cn

Received: 19 January 2015 / *Accepted:* 10 March 2015 / *Published:* 23 March 2015

Copper-doped lithium manganese spinel $LiCu_xMn_{2-x}O_4$ ($0 \leq x \leq 0.10$) as lithium ion cathode material were synthesized by a fameless combustion synthesis at 500 °C for 3 h, two-stage calcination at 600 °C for 3 h. The phase composition was determined by X-ray diffraction (XRD), which indicated that all samples exhibited a single spinel structure except that $LiCu_{0.08}Mn_{1.92}O_4$ had a little impurity of Mn_3O_4. Micro-morphology of the materials were characterized by scanning electron microscopy (SEM), suggesting particle size of samples was nearly uniform when copper-doped amount x ranged from 0 to 0.06, the particle of $LiCu_{0.08}Mn_{1.92}O_4$ and $LiCu_{0.10}Mn_{1.90}O_4$ more seriously agglomerated together than that of other samples. The cycle performance tests indicated that the sample $LiCu_{0.06}Mn_{1.94}O_4$ had the highest initial discharge specific capacity of 128.1 mA $h \cdot g^{-1}$ and the 150th capacity retention was 70.1% at 0.2 C rate. Cyclic voltammetry and electrochemical impedance spectroscopy of the sample $LiCu_{0.06}Mn_{1.94}O_4$ illustrated that appropriate copper-doped modification can improve electrochemical reversibility as well as suppress electrochemical impedance.

Keywords: Lithium ion cathode material; $LiCu_xMn_{2-x}O_4$; Copper-doped; Spinel $LiMn_2O_4$; a fameless combustion synthesis

1. INTRODUCTION

With the rapid demand growth of mobile portable devices and hybrid electric vehicles, lithium-ion batteries have been widely used as the most promising energy sources. Among the various materials, the spinel lithium manganese oxide not only has high specific energy, high voltage, stable discharge and pollution-free advantages, but also increases the speed of Li^+ ion insertion and

deinsertion during charging-discharging [1,2]. However, the capacity fade which have been attributed to Jahn-Teller distortion and Mn^{3+} dissolution has seriously suppressed its development. Doping is one of the effective ways to solve this problem, common elements include Co, Ni, Mg, Zn, Al [3-7]. The stability of the spinel structure has been improved by doping due to the reduced content of Mn^{3+}.

The copper-doped spinel materials $LiCu_xMn_{2-x}O_4$ were studied only by a few research groups in lithium ion batteries [8,9]. In addition, the preparation method is an important factor that affects the electrochemical performance of cathode materials, copper-doped methods mainly include solid-state reaction [10], sol-gel method [11,12], but these methods are hard to get single phase $LiMn_2O_4$ at low temperature in a short time. All these studies have shown that $LiCu_xMn_{2-x}O_4$ has a higher electronic conductivity, longer electrochemical cycle stability and better lithium ionic diffusivity than pristine $LiMn_2O_4$ [10-12]. This work adopts liquid-phase combustion synthesis method for the preparation of $LiMn_2O_4$ and copper-doped products [13]. This method uses flammable and oxidative salts as raw materials. Finally, obtain very fluffy products at low temperature in a short time. In our previous works, Al^{3+} and F^- have been successfully prepared doped $LiMn_2O_4$ [14,15], whose electrochemical performance have been effectively improved and single phase $LiMn_2O_4$ has been got.

2. EXPERIMENT

2.1 Preparation of materials

A series of $LiCu_xMn_{2-x}O_4$ ($0 \leq x \leq 0.10$) products were prepared by the liquid-phase combustion synthesis method. $LiNO_3$ (AR, Aladdin), $Mn(OAc)_2{\cdot}4H_2O$ (AR, Aladdin) and $Cu(CH_3COO)_2$ H_2O (AR, Tianjin Kemiou) were weighted into 300 mL crucibles according to a stoichiometric ratio of 1:(2-x):x (Li:Mn:Cu). Then joined the nitric acid and distilled water to make the the nitric acid concentration to 9 mol/L, and removed into an oven at 100 °C for several minutes to form the homogeneous solution. Next removed the homogeneous solution into a muffle furnace keeping temperature 500 °C for 3 h, cooled off to room temperature and grounded, then two-stage calcination at 600 °C for 3 h. Lastly, the target black powdery products obtained.

2.2 Characterization of the samples

The phase composition were identified by X-ray diffraction (XRD, D/max-TTRIII, Japan) with Cu-Kα radiation in a step of 0.02 ° over the range $10\ ° \leq 2\theta \leq 70\ °$ at an operation current of 30 mA and voltage of 40 kV , a scan speed of 4 °/min. Lattice parameters were acquired by means of Jade 5.0 software. The micro-morphology of the materials were analyzed by scanning electron microscopy (SEM, QUANTA 200, America FEI).

2.3 Electrochemical properties

The ectrodes were made by mixing active material, polyvinylidene fluoride (PVDF) and carbon black with a mass ratio of 8:1:1 in N-methyl-2-pyrrolidone (NMP) solvent in a ball-mill for 1.5 hours,

then the slurry was poured onto a clean aluminium foil by doctor-blade technology, drying in an oven at 80 °C for 4 h， cut into some disks with 16 mm diameter in the vacuum drying oven at 120 °C for 8 h for standby. The electrochemical properties were performed using CR2025 coin-type cells assembled in a glove box (MBraun, Germany) filled with high purity argon gas. Lithium metal foil, 1 M LiPF6 in EC/DMC (1:1 in volume) and Celgard 2320-type membrane were used as anode, electrolyte and separator, respectively. Electrochemical galvanostatical charge-discharge tests were carried out between 3.20-4.35 V (versus Li / Li^+) at 0.2 C by the Land electric test system CT2001A (Wuhan Jinnuo Electronic Co., Ltd). The cyclic voltammogram (CV) was performed on an Electrochemical Workstation (ZAHNER-elektrik GmbH & Co. KG, Kronach, Germany) from 3.6 to 4.5 V at a scan rate of 0.05 mV s^{-1}. All these tests were completed at room temperature.

3. RESULTS AND DISCUSSION

3.1 Structure and morphology of $LiCu_xMn_{2-x}O_4$

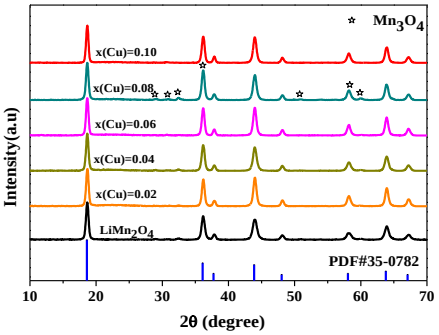

Figure 1. XRD patterns of $LiCu_xMn_{2-x}O_4$ ($0 \le x \le 0.10$)

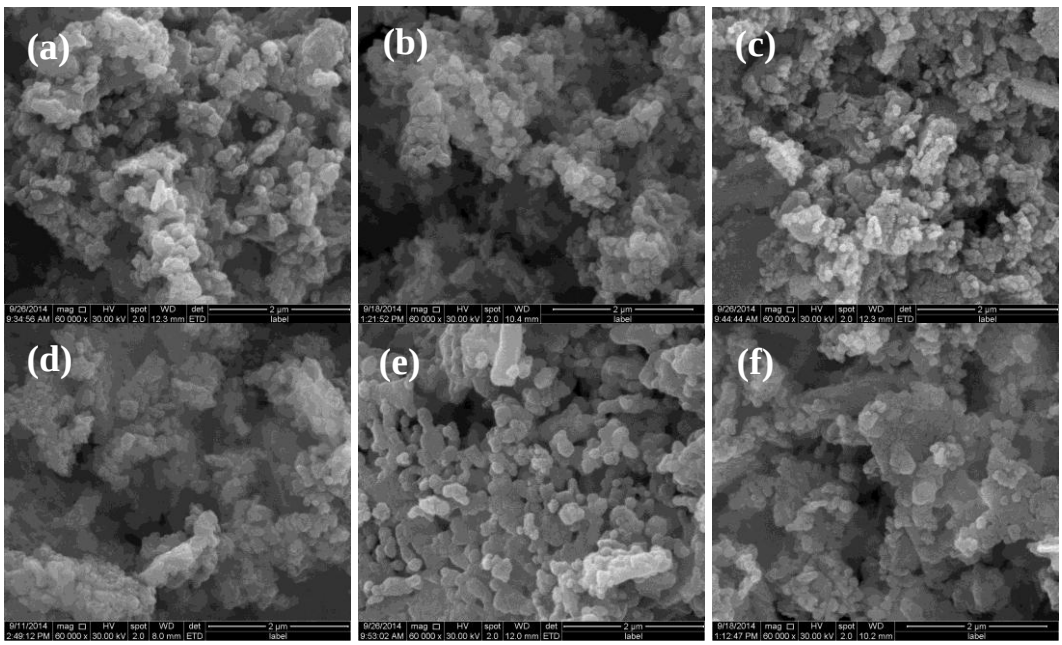

Figure 2. SEM images of $LiCu_xMn_{2-x}O_4$ (a:x=0, b:x=0.02, c:x=0.04, d:x=0.06, e:x=0.08, f:x=0.10)

As shown in Fig. 1, the XRD patters of all $LiCu_xMn_{2-x}O_4$ ($0 \le x \le 0.10$) samples correspond with the Fd3 m space group (PDF 35-0782) except that $LiCu_{0.08}Mn_{1.92}O_4$ had a little impurity of Mn_3O_4. In a ideal cubic spinel $LiMn_2O_4$, Mn^{3+} and Mn^{4+} ions averagely occupy the octahedral 16d sites, Li^+ ions and O^{2-} ions are located at the tetrahedral 8a sites and 32e sites [16]. That (2 2 0) peak around 2θ=30.7 ° don't exist indicating that copper ion don't replace tetrahedral 8a sites of spinel $LiMn_2O_4$, is likely to enter octahedral 16d sites to partially substitute the Mn^{3+} [17,18]. Furthermore, the intensity ratio of (3 1 1)/(4 0 0) peaks of product $LiCu_xMn_{2-x}O_4$ ($0 \le x \le 0.10$) are 0.917, 0.867, 0.936, 0.986, 0.829, 0.839, respectively, suggesting certain copper-doped materials improve stability of unit cell and present better electrochemical performances than prime [19].

Fig. 2 displays the SEM images of the $LiCu_xMn_{2-x}O_4$ ($0 \le x \le 0.10$) by a fameless combustion synthesis. Particle size is nearly uniform of about 200 nm, interface between particles becomes clear and porosity is larger when copper-doped amount ranges from 0 to 0.06, which indicates copper ion increasing the surface area of the electrochemical reaction. However, the sample $LiCu_{0.08}Mn_{1.92}O_4$ and $LiCu_{0.10}Mn_{1.90}O_4$ seriously agglomerated together, even appear to harden, which may suffer large resistance for Li^+ migration during charge-discharge course.

3.2 Galvanostatic cycling

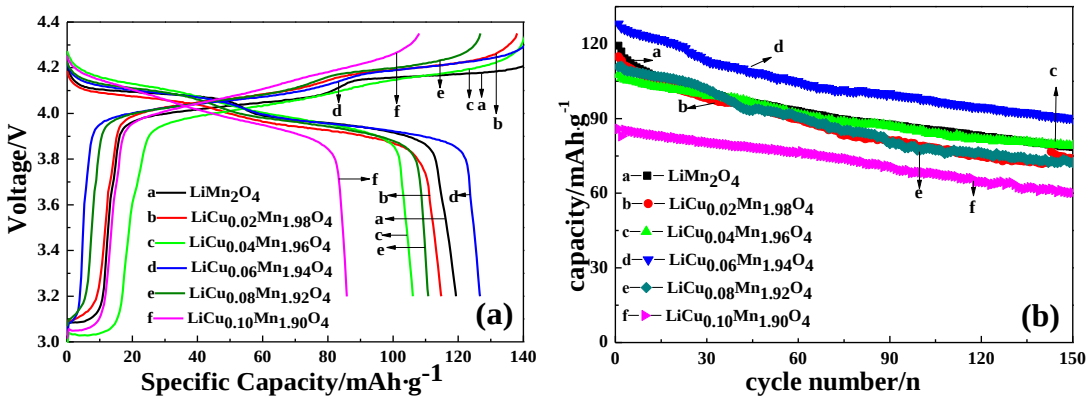

Figure 3. (a) First galvanostatic charge-discharge curves, (b) The discharge capacity vs. cycle number of the $LiCu_xMn_{2-x}O_4$ ($0 \le x \le 0.10$) at 0.2 C.

The initial charge-discharge curves of the $LiCu_xMn_{2-x}O_4$ ($0 \le x \le 0.10$) at 0.2 C rate in the voltage range of 3.20-4.35 V (vs. Li / Li^+). are shown in Fig 3(a). All products exhibit two evident potential plateaus at 3.90-4.26 V in accordance with Li/Li^+ extraction/insertion during charge-discharge cyclic curves. Fig 3(b) displays cycling performances of the $LiCu_xMn_{2-x}O_4$ ($0 \le x \le 0.10$), the $LiCu_{0.06}Mn_{1.94}O_4$ shows the highest initial discharge specific capacity of 128.1 mA h·g^{-1} as well as remains 89.9 mA h g^{-1}, much higher than other samples after 150 cycles. It is highly possible that copper ion partially substitute the Mn^{3+} at octahedral 16d sites leading to enhance the electrical conductivity [10,20]. The capacity retentions of the sample $LiCu_xMn_{2-x}O_4$ ($0 \le x \le 0.10$) are 65.8%, 64.4％, 73.5％, 70.1％, 65.2％, 69.2％ shown in Table 1, suggesting that electrochemical cycle

performance of spinel $LiMn_2O_4$ has been enhanced through appropriate copper-doped modification, which is due to the structure stability exhibited in Fig. 1.

Table 1. Discharge specific capacity and capacity retention of the $LiCu_xMn_{2-x}O_4$ ($0 \le x \le 0.10$)

Sample	Discharge specific capacity ($mA\ h \cdot g^{-1}$)		Capacity retention (%)
	First cycle	150th cycle	
$LiMn_2O_4$	119.3	78.5	65.8
$LiCu_{0.02}Mn_{1.98}O_4$	114.8	73.9	64.4
$LiCu_{0.04}Mn_{1.96}O_4$	107.6	79.1	73.5
$LiCu_{0.06}Mn_{1.94}O_4$	128.1	89.9	70.1
$LiCu_{0.08}Mn_{1.92}O_4$	110.8	72.3	65.2
$LiCu_{0.10}Mn_{1.90}O_4$	85.8	60.2	69.2

3.3 Cyclic voltammogram and electrochemical impedance

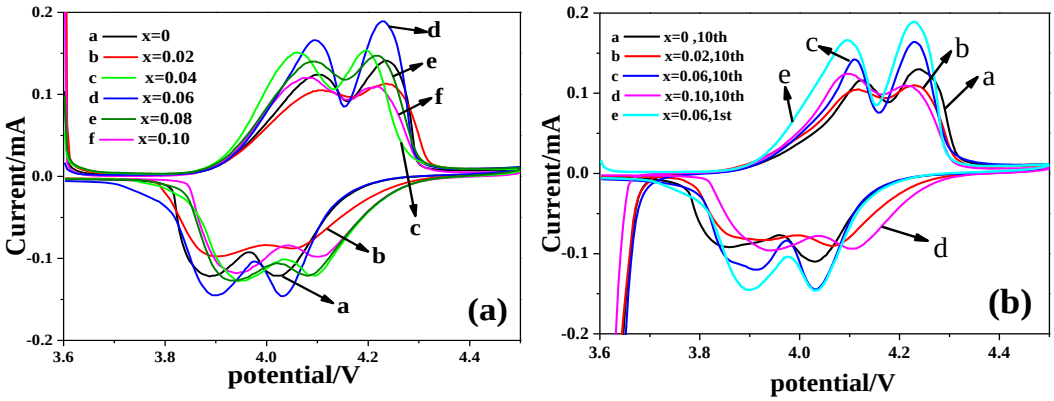

Figure 4. (a) the first CV curves of $LiCu_xMn_{2-x}O_4$ ($0 \le x \le 0.10$) measured at a scan rate of 0.05 mV s^{-1}, (b) the 10th cycle CV curves of samples

Fig. 4(a) depicts the first cyclic voltammograms (CV) of the sample $LiCu_xMn_{2-x}O_4$ ($0 \le x \le 0.10$) by a fameless combustion synthesis in the voltage range of 3.6-4.5 V at a scan rate of 0.05 mV s^{-1}. Obviously, two pairs of redox peaks are observed around at 4.08/3.90 V and 4.20/4.06 V, indicating Li/Li^+ extraction/insertion can be finished through a two-step process in consistent with two evident potential plateaus of the initial charge-discharge curve of the $LiCu_xMn_{2-x}O_4$ ($0 \le x \le 0.10$) in Fig 3(a) [21]. CV curves of the 10^{th} cycle of $LiCu_xMn_{2-x}O_4$ ($0 \le x \le 0.10$) measured at a scan rate of 0.05 mV s^{-1} shown in Fig 4(b). From the two profiles, we see the sample $LiCu_{0.06}Mn_{1.94}O_4$ has not only the highest peak current and peak potential but also the maximum peak area, which implies its lowest electrode polarization and highest Li^+ diffusion rate in the solid phase as well as a remarkable reversible electrochemical activity.

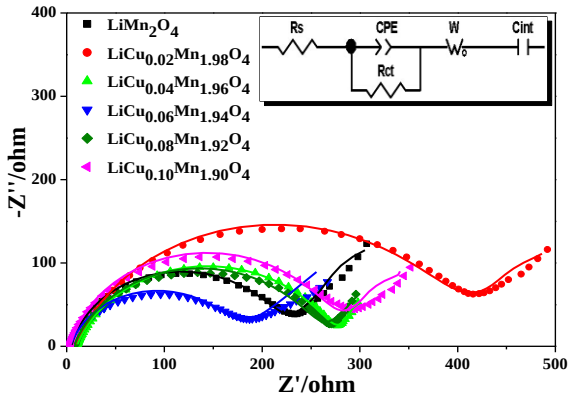

Figure 5. Niquist plots of $LiCu_xMn_{2-x}O_4$ ($0 \le x \le 0.10$) and Equivalent circuit of EIS.

The impedance spectra and equivalent circuit diagram of the sample $LiCu_xMn_{2-x}O_4$ ($0 \le x \le 0.10$) was shown in Fig. 5. Rs , Rct and CPE represent solution resistance, the charge-transfer resistance and the double layer capacitance, Cint reflects the Li^+ intercalation capacitance, the low-frequency lines are the Li^+ diffusion resistance in the solid phase of spinel structure, namely Warburg impedance.

Table 2. The characteristic values of electrochemical parameters of EIS.

Sample	$LiMn_2O_4$	$LiCu_{0.02}Mn_{1.98}O_4$	$LiCu_{0.04}Mn_{1.96}O_4$	$LiCu_{0.06}Mn_{1.94}O_4$	$LiCu_{0.08}Mn_{1.92}O_4$	$LiCu_{0.10}Mn_{1.90}O_4$
Rs (Ω)	4.61	8.69	10.20	3.26	7.34	3.45
Rct (Ω)	213.1	389.7	265.2	163.2	250.7	268.0

Table 2 lists the R_s and R_{ct} of the sample $LiCu_xMn_{2-x}O_4$ ($0 \le x \le 0.10$), the $LiCu_{0.06}Mn_{1.94}O_4$ delivers the lowest value of 3.26 Ω, 163.2 Ω than the pure $LiMn_2O_4$ and other copper-doped samples, suggesting that the $LiCu_{0.06}Mn_{1.94}O_4$ lowering dissolution than that of $LiMn_2O_4$ and other samples. The result suggests proper copper-doped products enhance the Li^+ intercalation/de intercalation procedure during charge-discharge process of lithium ion battery [22], corresponding to the SEM in Fig. 2.

4. CONCLUSION

In summary, the $LiCu_xMn_{2-x}O_4$ ($0 \le x \le 0.10$) were successfully synthesized by a fameless combustion synthesis calcined at 500 °C for 3 h, two-stage calcination at 600 °C for 3 h. The crystalline of the samples got improved except $LiCu_{0.08}Mn_{1.92}O_4$. The particle size of the $LiCu_xMn_{2-x}O_4$ whose copper-doped amount x ranged from 0.02 to 0.06 was close to that of the undoped spinel $LiMn_2O_4$, while the samples $LiCu_{0.08}Mn_{1.92}O_4$ and $LiCu_{0.10}Mn_{1.90}O_4$ became larger. Among the synthesized materials, the $LiCu_{0.06}Mn_{1.94}O_4$ had the highest initial discharge specific capacity of 128.1 mA h g^{-1} and the 150th discharge capacity of 89.9 mA h g^{-1}, capacity retention was 70.1% at 0.2 C rate. The initial discharge specific capacity of the pristine $LiMn_2O_4$ was 119.3 mA h g^{-1} and remained 78.5

mA h g^{-1} after 150 cycles, capacity retention was 65.8% at 0.2 C rate. The charge transfer resistance of the $LiCu_{0.06}Mn_{1.94}O_4$ electrode was the lowest, suggesting that the sample $LiCu_{0.06}Mn_{1.94}O_4$ can effectively promote electrode kinetic activity.

ACKNOWLEDGEMENTS
This work was financially supported by the National Natural Science Foundation of China (51262031, 51462036), Program for Innovative Research Team (in Science and Technology) in University of Yunnan Province (2011UY09), Yunnan Provincial Innovation Team (2011HC008), the Natural Science Foundation of Yunnan Provincial Education Department (2014J079), and Innovation Program of Yunnan Minzu University (2013HXSRTY01, 2014YJZ10, 2014YJY74).

References

1. R M Mohan, C. Liebenow and M. Jayalakshmi, *J. Electrochem Solid St.* 5 (2001) 348-354.
2. Y. Z. Wang, X. Shao , H. Y. Xu , M. Xie , S. X. Deng , H. Wang , J. B. Liu and H. Yan, *J. Power Sources.* 226 (2013) 140-148
3. Z. J. Wang, J. L. Du, Z. L. Li and Z. W, *Ceram Int.* 40 (2014) 3527–3531.
4. F. D. Yu, Z. B. Wang, F. Chen, J. Wu, X. G. Zhang and D. M. Gu, *J. Power Sources.* 262 (2014) 104-111
5. M. W. Xiang, C. W. Su, L. L. Feng, M. L. Yuan and J. M. Guo, *Electrochim Acta.* 25 (2014) 524-529
6. D. Arumugam, G. P. Kalaignan, K. Vediappan and C. W, *Electrochim Acta.* 55 (2010) 8439–8444
7. Y.J. Wei, K. W. Nam, K. B. Kim and G. Chen. *Solid State Ionics.* 177 (2006) 29-35.
8. Ein Eli Y and Howard W F. *J. Electrochem Soc.* 144 (1997) L205-L207.
9. Ein Eli Y and Howard W F and Lu S H, *J. Electrochem Soc.*145 (1998) 1238-1244.
10. J. Molenda, J. Marzec, K. Swierczek, W. Ojczyk, M. Ziemnicki, M. Molenda, M. Drozdek and R. Dziembaj, *Solid State Ionics.* 171 (2004) 215-227.
11. M. C Yang, B. Xu and J. H. Cheng, *Chemistry of Materials.* 23(11) (2011) 2832-2841.
12. R. Thirunakaran, B. R. Babu. and N. Kalaiselvi, *Bulletin of Materials Science.* 24(1) (2001) 51-55.
13. M. M. Chen, X. Y. Zhou, X. Z. Huang, M. Huang, C. W. Su, J. M. Guo and Y. J. Zhang, *Advanced Materials Research.* 581 (2012) 611-615.
14. M. W. Xiang, X. Y. Zhou, Z. F. Zhang, M. M. Chen, H. L. Bai and J. M. Guo, *Advanced Materials Research.*652-654 (2013) 891-895
15. M. M. Chen, X. Y. Zhou, C. W. Su, M. W. Xiang and J. M. Guo, *Asian J. Chem.* 26 (2014) 714-718.
16. M. Prabu, M. V. Reddy, S. Selvasekarapandian, G. V. Subba Rao and B.V.R. Chowdari, *Electrochim. Acta.* 88 (2013) 745.
17. J. L. Wang, Z. H. Li and J. Yang, *Electrochim Acta.*75 (2012) 115-122.
18. Doretta Capsoni, Marcella Bini, Gaetano Chiodelli, Vincenzo Massarotti, Maria Cristina Mozzati and Carlo B. Azzoni, *Solid State Communications.* 125 (2003) 179-183.
19. J. L. Wang, Z. H. Li and J. Yang, *Electrochim Acta.* 75 (2012) 115-122.
20. C. H. Zheng, Z. F. Wu, J. C. Li, X. Liu and D. L. Fang, *Ceram Int.* l40 (2014) 8455–8463.
21. Y. Y. Xia and M. Yoshio, *J.Electrochem.Soc.*143 (1996) 825–833.
22. L. L. Xiong, Y. L. Xu and T. Tao, *J. Power Sources.* 199 (2012) 214– 219